Enhanced $B_q \to \ell\ell'$ and $B \to (K,\pi)\ell\ell'$ in light of $(g-2)_\mu$

Wei-Shu Hou, Girish Kumar, and Sven Teunissen
Department of Physics, National Taiwan University, Taipei 10617, Taiwan

(Received 10 September 2022; accepted 24 April 2023; published 15 May 2023)

We study lepton flavor violating (LFV) B decays in a general two Higgs doublet model with sub-TeV exotic scalars. Two different parameter spaces are explored: one dominated by extra top Yukawa coupling ρ_{tt}, the other by LFV couplings relevant for the muon $g-2$ anomaly. In the first case, flavor constraints such as $\ell \to \ell'\gamma$, $h \to \ell\ell'$ imply LFV B decays are far below experimental sensitivities. The second case needs to be close to the alignment limit, but $B_q \to \tau\mu$ and $B \to (K,\pi)\tau\mu$ rates can lie within the sensitivities of Belle II and LHCb Upgrade II. Neutral B meson mixings and $B, K, \pi \to \ell\nu$ decays provide important flavor constraints on parameter space. B decays involving e–τ violation are constrained by $\mu \to e$ processes.

DOI: 10.1103/PhysRevD.107.095017

I. INTRODUCTION

Flavor changing neutral couplings (FCNCs) in the Standard Model (SM) occur only beyond tree-level and the corresponding rates are small due to suppression from GIM mechanism [1] and vanishing neutrino masses. But new physics (NP) beyond SM could have interactions that allow for sizable FCNC processes. Therefore, the precise measurements of rare FCNC decays serve as powerful probes of physics beyond SM. In this context, rare B decays offer excellent opportunities as, in addition to loop factors, these are suppressed further by small CKM factors, while the b quark mass is sufficiently large so long- and short-distance effects can be separated and extracted with reasonable precision.

Rare leptonic decays of B mesons are advantageous for study, as all hadronic effects are contained in the decay constant, calculable by lattice QCD [2], hence the decay rates can be predicted with great precision. On the experimental front, there has been excellent progress with ever increasing precision. One example is the helicity-suppressed rare $B_s \to \mu^+\mu^-$ decay, which provides one of the most sensitive probes of scalar NP interactions.

Based on full Run 1 and Run 2 data with 9 fb^{-1} luminosity, LHCb [3,4] reported the branching ratio,

$$\mathcal{B}(B_s \to \mu\mu) = (3.09^{+0.46+0.15}_{-0.43-0.11}) \times 10^{-9}, \qquad \text{[LHCb]} \qquad (1)$$

Subsequently, CMS [5] announced their Run 2 result,

$$\mathcal{B}(B_s \to \mu\mu) = (3.83^{+0.38+0.19+0.14}_{-0.36-0.16-0.13}) \times 10^{-9}, \quad \text{[CMS]} \qquad (2)$$

based on 2016-2018 data with 140 fb^{-1} integrated luminosity. The central values of LHCb and CMS results differ by 1.2σ, and lie on opposite sides of SM expectation, $\mathcal{B}(B_s \to \mu^+\mu^-)_{\rm SM} = (3.66 \pm 0.14) \times 10^{-9}$ [6,7]; but within errors, both measurements agree with SM, thereby provide strong bounds on NP interactions. The CKM suppressed $B_d \to \mu^+\mu^-$ is not measured yet. The current 95% C.L. upper limit $\mathcal{B}(B_d \to \mu^+\mu^-) < 1.9 \times 10^{-10}$ [5] is still above the SM prediction at $\mathcal{B}(B_d \to \mu^+\mu^-)_{\rm SM} = (1.03 \pm 0.05) \times 10^{-10}$ [7].

A more exquisite probe to hunt for NP is provided by lepton flavor violating (LFV) decays of B mesons. Since LFV phenomena is practically absent in SM, any experimental detection will be unambiguous signals for NP. *BABAR*, Belle, and more recently LHCb have searched for LFV B decays; no evidence so far has been observed, which provide stringent limits. In Table I we list current bounds, together with projected sensitivities in the near future on promising LFV B decays.[1]

In this article, we explore the possible size of LFV B decays associated with $b \to q\ell\ell'(q = s, d)$ in one of the simplest extensions of SM, the general two Higgs doublet model (g2HDM) [21] (for a review of 2HDMs, see [22]), sometimes denoted as 2HDM Type III [23], where the Lagrangian itself contains flavor changing neutral couplings of exotic scalar bosons, denoted as ρ_{ij} (which are

[1]We note in passing that in certain NP scenarios (e.g., those considered in Refs. [8–10]) lepton flavor nonuniversality can also lead to lepton flavor violation in B decays. However, LHCb recently reported [11,12] measurements concerning the latter, finding no evidence of lepton universality breaking in $b \to s\ell^+\ell^-$ decays.

defined in Eq. (3) later). In our study, we investigate two very different parameter space choices motivated by different phenomenological reasons. In the first case, the NP Yukawa matrices are somewhat SM-like in strength; the largest coupling, just as in SM, is the top-related diagonal coupling $\rho_{tt} \lesssim \lambda_t$, where $\lambda_t = \sqrt{2}m_t/v$ is the SM top Yukawa coupling. Another assumption, supported by experiment [24], is of small but finite mixing, denoted as $c_\gamma (\equiv \cos\gamma)$, between CP even scalars in the model (alignment). It was shown [25] that lepton-related NP couplings $\rho_{\ell\ell'}$ are constrained to be small, due to bounds from $h \to \ell\ell'$ decay and $\mu \to e$, $\tau \to \mu$ LFV processes. Driven by ρ_{tt} (or ρ_{tc}), this scenario can realize electroweak baryogenesis (EWBG) for explaining the baryon asymmetry of the Universe (BAU) [26,27], providing strong motivation for experimental exploration.

In the second case, we adopt the alignment limit of $c_\gamma \to 0$, which then allows for sizable NP lepton Yukawa couplings related to μ–τ sector. This scenario is usually invoked for NP explanation of the anomalous magnetic moment of muon, $(g-2)_\mu$, recently affirmed by Muon g-2 collaboration [28]. In this scenario, as opposed to the first case, in order to satisfy bounds from LHC direct search for $gg \to \phi \to \tau\mu$ and the flavor bound of $\tau \to \mu\gamma$ [29], the ρ_{tt} coupling cannot be substantial. After evaluating constraints from neutral B_q mixing and H^+-induced leptonic decays of B, K, π, we identify parameter space that can lead to significantly large rates of LFV B decays, which are within reach of upcoming measurements. Though we mostly focus on flavor violation in the μ–τ sector, we will present g2HDM expectations for flavor violation in μ–e and τ–e sectors as well.

This article is organized as follows. In Sec. II we introduce the g2HDM Lagrangian and set up our notation. In Sec. III, we discuss Case I; after discussing bounds on ρ_{tt} from $B_q \to \mu\mu$ and B_q mixing, we present our results for LFV B decays. In Sec. IV, we discuss Case II by first revisiting the one-loop solution to $(g-2)_\mu$ in g2HDM; after discussing the main constraints on relevant couplings, we present our results for LFV B decays. Finally, in Sec. V, we present our conclusions.

II. NEW YUKAWA INTERACTIONS

Adding a second Higgs doublet to the SM gives four new Higgs bosons, the neutral scalars H, A, and charged Higgs boson $H^\pm$ in mass basis. In the limit of CP conserving scalar potential, the $H(A)$ boson is CP-even (odd). Due to absence of discrete Z_2 symmetry on Yukawa sector, it is not possible to diagonalize simultaneously the Yukawa matrices associated with the two Higgs doublets. As a result, the Yukawa Lagrangian of g2HDM contains Higgs FCNCs, giving rise to flavor violation at tree-level. Working in the so-called Higgs basis [30–32], the Yukawa Lagrangian in g2HDM is given by [33,34],

$$\begin{aligned}\mathcal{L} = &-\frac{1}{\sqrt{2}}\sum_{f=u,d,\ell}\bar{f}_i[(\lambda_i^f\delta_{ij}s_\gamma + \rho_{ij}^f c_\gamma)h \\ &+ (\lambda_i^f\delta_{ij}c_\gamma - \rho_{ij}^f s_\gamma)H - i\mathrm{sgn}(Q_f)\rho_{ij}^f A]Rf_j \\ &- \bar{u}_i[(V\rho^d)_{ij}R - (\rho^{u\dagger}V)_{ij}L]d_j H^+ \\ &- \bar{\nu}_i\rho_{ij}^\ell R\ell_j H^+ + \text{H.c.}, \end{aligned} \tag{3}$$

where indices i, j denote the generation of fermion f, Q_f the corresponding electric charge, and $R(L) = (1 \pm \gamma_5)/2$ are chiral projections. Note that NP Yukawa matrices ρ^f are in general not Hermitian, hence elements ρ_{ij} can have arbitrary complex phases.

The presence of tree-level Higgs FCNCs lead to potentially dangerous flavor violating decays of SM Higgs boson, $h \to f_i f_j (i \neq j)$, which are severely bound by experiments. To evade such constraints, usually some Z_2 symmetry is imposed on NP Yukawa sector to enforce the natural flavor conservation condition [35]. However, the vertex hf_if_j in g2HDM is proportional to the mixing angle c_γ, therefore with suppression due to sufficiently small c_γ, as hinted by current Higgs data [24], the mere existence of Higgs FCNCs in g2HDM is not directly a cause of concern. But, of course, the strength of Higgs FCNC couplings will be determined by data.

The scalar potential can be found, e.g., in Ref. [36]. For our study, besides Eq. (3), we only need physical H, A, and H^+ masses as benchmarks. We focus on sub-TeV masses in range of [300, 500] GeV and take $m_A = m_{H^+}$, usually adopted[2] to evade constraint from T parameter (constraints from S and U parameters are easily satisfied [42,43]), where the formula for T in g2HDM is given in Appendix. In addition to oblique parameters, the parameter space considered in Secs. III and IV satisfy [29,44] perturbativity, unitarity, and positivity.

III. CASE I: TOP YUKAWA DOMINANCE

We assume that NP top coupling $\rho_{tt} \sim \lambda_t$ is the largest coupling. This assumption finds support also from the Cheng-Sher ansatz [45], $\rho_{ij} \propto \sqrt{m_i m_j}/v$, frequently employed to control tree-level Higgs FCNC. But as mentioned in the preceding section, small c_γ can tackle the issue of Higgs FCNC, so we do not quite follow the ansatz. We take $c_\gamma \sim 0.1$ as sample value, but note that due to ρ_{tt} being the dominant quark coupling, the main g2HDM contribution to $b \to q\ell\ell^{(\prime)}$ processes are induced by H^+

[2]Recent M_W measurement by CDF [37] shows significant tension with SM, as well as measurements by other experiments. The CDF value can be explained in g2HDM (see, for example, Refs. [38–41]) by inducing NP contribution to T parameter. This, however, would necessarily require the masses of exotic scalars to be nondegenerate. Given the current situation is unclear, we do not consider accounting for the CDF result.

interactions that do not depend on c_γ. The c_γ value is relevant for constraints from $h \to \ell\ell'$.

The leading flavor constraints on ρ_{tt} are from B physics discussed later in detail. For LFV B decays, we also need to determine the strength of lepton couplings $\rho_{\ell\ell'}$. We have discussed previously [25] the allowed strength of ρ^ℓ for large ρ_{tt}, so let us give a brief summary. For finite c_γ, $h \to \ell\ell'$ provide important constraints on $\rho_{\ell\ell'}$, independent of ρ_{tt}. For example, the current upper limit on $h \to \tau\mu$ from CMS, based on full Run 2 data [46],

$$\mathcal{B}(h \to \tau\mu) < 0.15\% \qquad (95\%\ \text{C.L.}) \tag{4}$$

implies $|\rho_{\tau\mu} c_\gamma| < 0.1\lambda_\tau$ for $\rho_{\tau\mu} = \rho_{\mu\tau}$, giving $\rho_{\tau\mu} \sim \lambda_\tau$ for $c_\gamma = 0.1$ (see Appendix for expressions in g2HDM). Even if $c_\gamma \sim 0$ so the $h \to \tau\mu$ bound of Eq. (4) can be evaded, μ–τ couplings together with sizable ρ_{tt} unavoidably generate $\tau \to \mu\gamma$ at two-loop via Barr-Zee diagrams [47]. The recently updated bound of $\tau \to \mu\gamma < 4.2 \times 10^{-8}$ [48] from Belle again gives $\rho_{\tau\mu} \sim \mathcal{O}(\lambda_\tau)$ for $\rho_{tt} \sim \lambda_t$ and $m_{H,A} \sim 300$ GeV.

The current upper limits on the τ–e sector, e.g. $h \to \tau e$ [46] and $\tau \to e\gamma$ [49] give relatively weak bounds, but couplings related to e–μ are strongly constrained by $\mu \to e\gamma$. The MEG bound $\mu \to e\gamma < 4.2 \times 10^{-13}$ [50] gives $\rho_{\mu e}\rho_{tt} \lesssim 0.4\lambda_e\lambda_t$ for $m_{H,A} \sim 300$ GeV [51]. This again suggest that for $\rho_{tt} \sim \lambda_t$, strengths of μ–e flavor violating couplings are similar to SM electron Yukawa, λ_e. Concerning flavor conserving $\rho_{\ell\ell}$, measurements related to $h \to \mu\mu$ [52,53] and $h \to \tau\tau$ [54] imply that, for $c_\gamma \sim 0.1$, strengths of $\rho_{\mu\mu}$ and $\rho_{\tau\tau}$ are close to $\mathcal{O}(\lambda_\mu)$ and $\mathcal{O}(\lambda_\tau)$, respectively [55]. A very important insight concerning the strength of ρ_{ee} came in Ref. [27], where it was uncovered that, to evade constraints from electric dipole moment of electron measured by ACME [56,57], ρ_{tt} and ρ_{ee} should follow the pattern of $|\rho_{ee}/\rho_{tt}| \propto \lambda_e/\lambda_t$, again echoing SM-like strength for ρ_{ee}.

With discussion as delineated above, we take the following structure for NP lepton Yukawa matrix ρ^ℓ [25],

$$\rho_{\ell\ell} \lesssim \mathcal{O}(\lambda_\ell); \quad \rho_{e\ell} \lesssim \mathcal{O}(\lambda_e); \quad \rho_{\tau\ell'} \lesssim \mathcal{O}(\lambda_\tau) \quad (\ell' \neq e), \tag{5}$$

which will be our working assumption in estimating rates of LFV B decays in Case I.

The NP contribution to $b \to q\ell\ell^{(\prime)}$ due to ρ_{tt} arise from one-loop diagrams shown in Fig. 1, where the Z-penguin diagram dominates. The diagrams generate the following effective Hamiltonian,

$$-\mathcal{H}_{\text{eff}} = C_V[\bar{q}\gamma_\mu L b][\bar{\ell}\gamma^\mu \ell^{(\prime)}] + C_A[\bar{q}\gamma_\mu L b][\bar{\ell}\gamma^\mu\gamma_5 \ell^{(\prime)}], \tag{6}$$

contributing to both axial and vector coefficients,

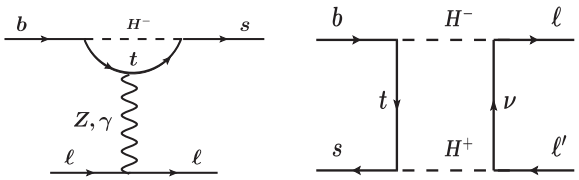

FIG. 1. H^+-induced Feynman diagrams for $b \to s\ell\ell$.

$$C_A^Z = \frac{V_{tq}^* V_{tb} |\rho_{tt}|^2}{16\pi^2 v^2} G_Z(x_t), \quad C_V^Z = -(1 - 4s_W^2) C_A^Z, \tag{7}$$

while γ-penguin contributes only to vector coefficient,

$$C_V^\gamma = -\frac{e^2 V_{tq}^* V_{tb} |\rho_{tt}|^2}{16\pi^2 m_{H^+}^2} G_\gamma(x_t), \tag{8}$$

where $x_t = m_t^2/m_{H^+}^2$, s_W is Weinberg angle and $G_{\gamma,Z}(x)$ are $t - H^+$ loop functions given in Appendix. Note that contributions in Eq. (7) and (8) are universal to all lepton flavors due to SM vertex on lepton end, and therefore only affect lepton flavor conserving B decays.

The box diagram in Fig. 1, however, does depend on lepton flavor and will contribute to LFV B decays (box diagram with $W^+ - H^+$ in the loop depends on the down-type couplings and therefore does not contribute). The corresponding Wilson coefficients are given by [58],

$$C_V^{\text{box}} = C_A^{\text{box}} = \frac{-V_{tq}^* V_{tb} |\rho_{tt}|^2 \rho_{i\ell}^* \rho_{i\ell'}}{128\pi^2 m_{H^+}^2} [1 + 2G_Z(x_t)]. \tag{9}$$

Before discussing numerical results, let us discuss briefly constraints on ρ_{tt} from the flavor conserving decays $B_q \to \mu\mu$ and neutral B_q mixings, which will help us determine the upper limit of ρ_{tt} from data for a given value of m_{H^+}. For numerical analysis, we use the open-source packages FLAVIO [59] and WILSON [60] for calculating flavor observables and QCD running of Wilson coefficients from NP scale to physical low-energy processes.

In Fig. 2, we give the region ruled out at 95% C.L. in ρ_{tt}–m_{H^+} plane for both LHCb [3,4] (orange) and CMS [5] (green) measurements of $B_s \to \mu\mu$. It is interesting to note that, though the central value of the latest CMS measurement is closer to the SM prediction of $(3.66 \pm 0.14) \times 10^{-9}$, the resulting constraint on ρ_{tt} is weaker compared to that from LHCb. This is because only the axial vector coefficient C_A^Z modifies $B_s \to \mu\mu$ (see Appendix) with the following correction,

$$\frac{\mathcal{B}(B_s \to \ell\ell)}{\mathcal{B}(B_s \to \ell\ell)_{\text{SM}}} \approx [1 - 1.2|\rho_{tt}|^2 G_Z(x_t)]^2, \tag{10}$$

with $G_Z(x) < 0$. Since there is no sensitivity to $\arg \rho_{tt}$, $B_s \to \mu\mu$ rate can only be enhanced, so the central value of CMS

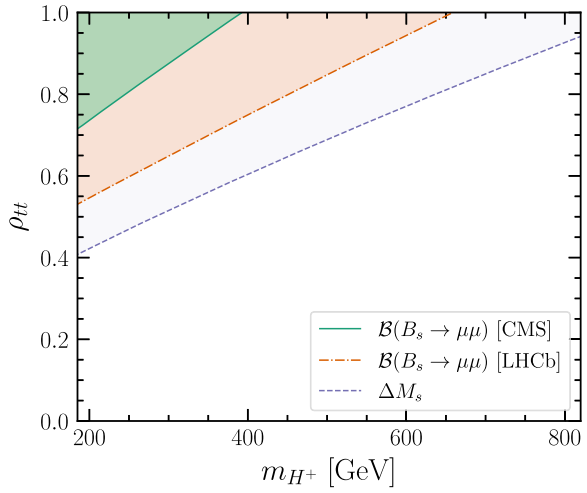

FIG. 2. Constraints in $\rho_{tt} - m_{H^+}$ plane from B physics.

being on the higher side of SM allows for relaxed constraint on ρ_{tt}. Note also that, since Eq. (10) does not depend on CKM elements, the result holds true for $B_d \to \ell\ell$ as well. The current measurements for $B_q \to ee, \tau\tau$ [24] are rather poor, therefore no improved constraint can be obtained. For $\rho_{tt} \sim 0.5$ and $m_{H^+} = 300$ GeV, Eq. (10) implies that the rates of all $B_q \to \ell\ell$ get enhanced by ~10% over their SM value, which fits the rising experimental trend.

A better constraint can be obtained from neutral B_q mixings. The $\Delta B = \Delta S = 2$ transitions arise from H^+ box diagrams of Fig. 3, which generate [58],

$$\mathcal{H}_{\text{eff}} = (C_1^{HH} + C_1^{WH})[\bar{s}\gamma^\mu Lb][\bar{s}\gamma^\mu Lb] + \text{H.c.}, \quad (11)$$

where C_1^{HH} is from H^+–H^- diagrams,

$$C_1^{HH} = -\frac{V_{ts}^{*2} V_{tb}^2 |\rho_{tt}|^4}{128\pi^2 m_{H^+}^2} f(x_t), \quad (12)$$

and C_1^{WH} from W^+–H^- diagrams,

$$C_1^{WH} = \frac{V_{ts}^{*2} V_{tb}^2 m_t^2 |\rho_{tt}|^2}{32\pi^2 v^2 m_W^2} g(y, x_t), \quad (13)$$

with $y = m_W^2/m_{H^+}^2$, and loop functions $f(x)$, $g(x)$ are given in Appendix. Similar expressions for B^0 mixing are obtained by replacing $s \to d$ in Eqs. (12) and (13). The current values of mass differences ΔM_q are [24],

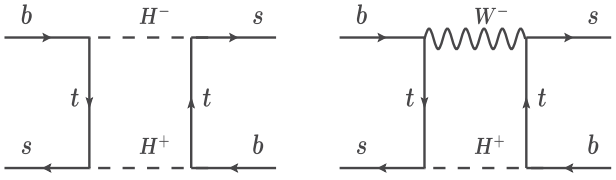

FIG. 3. H^+-induced Feynman diagrams for neutral B mixing.

$$\Delta M_{B_s} = (17.741 \pm 0.020)\ \text{ps}^{-1}, \quad (14)$$

$$\Delta M_{B_d} = (0.5065 \pm 0.0019)\ \text{ps}^{-1}, \quad (15)$$

whereas SM predictions are $\Delta M_{B_s} = (18.4^{+0.7}_{-1.2})\ \text{ps}^{-1}$ and $\Delta M_{B_d} = (0.533^{+0.022}_{-0.036})\ \text{ps}^{-1}$ [61].

In Fig. 2, the ΔM_s constraint (light purple) is shown in ρ_{tt}–m_{H^+} plane, which gives the leading constraint on ρ_{tt}. The constraints from B^0 mixing, as well as from $b \to s\gamma$ (see Appendix for relevant NP contribution), are relatively weak and not shown. Note also that, after replacing external fermion lines $\{bs\} \to \{sd\}$ in Fig. 3, these box diagrams will contribute to neutral kaon mixing and modify mixing parameters ΔM_K and ε_K [24], but the resulting constraints [62] on ρ_{tt} are not competitive with B_s mixing.

We find that $\rho_{tt} \sim 0.5$ is a reasonable choice with scalar mass spectrum in [300, 500] GeV range. With lepton couplings from Eq. (5), we can now estimate various LFV B branching ratios. As discussed, both Z- and γ-penguins preserve lepton flavor, and only box diagrams of Fig. 1 contribute. But this contribution is rather suppressed by small $\rho_{\ell\ell'}$. For $\rho_{tt} = 0.5$ and $m_{H^+} = 300$ GeV, we find,

$$\mathcal{B}(B_s \to \mu\tau) \simeq 3 \times 10^{-18}, \qquad \mathcal{B}(B_d \to \tau\mu) \simeq 10^{-19}, \quad (16)$$

with $B_q \to e\tau, e\mu$ further suppressed due to smaller electron Yukawa couplings. We therefore find that LFV B decays will be far below future sensitivities in Table I in g2HDM for Case I, with semileptonic decays $B \to (K, \pi)\ell\ell'$ analogously suppressed.

IV. CASE II: μ–τ YUKAWA DOMINANCE

The weakness of $\rho_{\ell\ell'}$ in Eq. (5), together with GIM suppression, do not allow large LFV effects in Case I, but instead constrains ρ_{tt} through $B_s \to \mu\mu$ and B_s mixing. Now we explore a scenario where the LFV μ–τ couplings can be sizable. One motivation for such parameter space is to address the disagreement between SM prediction and experimental measurement of the anomalous magnetic moment of the muon, $a_\mu = (g-2)_\mu/2$.

Recently, the Fermilab Muon g-2 experiment [28] reported its first measurement of a_μ. Combined with the previous result of Brookhaven [63], the result of $a_\mu^{\text{Exp}} = 116592061(41) \times 10^{-11}$ [28] compared to the theory consensus value of $a_\mu^{\text{SM}} = 116591810(43) \times 10^{-11}$ [64–85] is larger by more than 4σ [28][3]

$$\Delta a_\mu = a_\mu^{\text{Exp}} - a_\mu^{\text{SM}} = (251 \pm 59) \times 10^{-11}. \quad (17)$$

[3]The SM prediction of $(g-2)_\mu$ based on the recent lattice results [86–90] is closer to the experimental value. However, the low energy data on $\sigma(e^+e^- \to \text{hadrons})$ [91–93] show tension with these lattice results, which calls for further investigation. In this paper we will take Eq. (17) as evidence of NP.

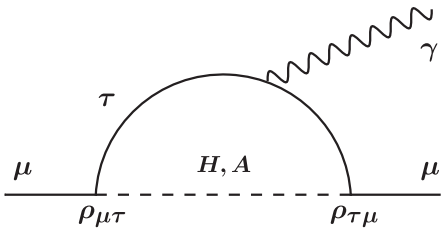

FIG. 4. One-loop diagram for $(g-2)_\mu$.

The difference can be explained in g2HDM via one-loop diagram[4] given in Fig. 4, which in the limit of $c_\gamma \to 0$ gives the following NP correction [43,96,97],

$$\Delta a_\mu|_\phi \simeq \frac{m_\mu m_\tau \mathrm{Re}(\rho_{\tau\mu}\rho_{\mu\tau})}{16\pi^2 m_\phi^2}\left[\log\frac{m_\phi^2}{m_\tau^2} - \frac{3}{2}\right], \tag{18}$$

for each $\phi = H,\ A$. The total contribution is $\Delta a_\mu = (\Delta a_\mu)_H - (\Delta a_\mu)_A$ as H and A effects are opposite in sign. Therefore, to obtain a finite Δa_μ, H and A must be nondegenerate: $\Delta m = m_A - m_H \neq 0$.

To present our numerical results, we follow Ref. [29] and assume H to be lighter, setting $m_H = 300$ GeV. For Δm, we take two choices for illustration: 40 and 200 GeV. The small $\Delta m = 40$ GeV implies large cancellation between H and A contributions, and therefore a larger value of $\rho_{\tau\mu} \sim 30\lambda_\tau$ (we implicitly assume $\rho_{\tau\mu} = \rho_{\mu\tau}$) is required to account for difference in Eq. (17) within 1σ solution. For larger Δm case, cancellation between H and A becomes mute since effect of heavy A starts to decouple, and one only needs a smaller $\rho_{\tau\mu} = \rho_{\mu\tau} \sim 20\lambda_\tau$.

With strength of $\rho_{\tau\mu}$ more than an order larger than Case I [compare Eq. (5)], the experimental bound of Eq. (4) implies $c_\gamma \sim 0.005$ or smaller. We therefore set $c_\gamma = 0$ to simplify (which would demand some yet unknown symmetry). Another important implication of large $\rho_{\tau\mu}$ is smallness of ρ_{tt} [29], because of bound from $\tau \to \mu\gamma$ [48]. In fact, a more stringent constraint on ρ_{tt} can be set [29] by the collider search for $gg \to H, A \to \tau\mu$ [98]. Therefore, if muon $g-2$ arises from one-loop in g2HDM, ρ_{tt} is unavoidably small.

One possibility for enhancing LFV B decays in g2HDM is to allow the ρ^d Yukawa matrix to be nondiagonal. Explicitly, if one allows for finite ρ_{bq} and ρ_{qb} for $q = s,\ d,\ b \to q\ell\ell^{(\prime)}$ is at tree level while $B_q \to \ell\ell$ do not suffer helicity suppression. The effective Hamiltonian is,

$$\mathcal{H}_{\mathrm{eff}} = -(C_S O_S + C_P O_P + C_S' O_S' + C_P' O_P'), \tag{19}$$

where $\mathcal{O}_S = (\bar{s}Rb)(\bar{\ell}\ell')$, $\mathcal{O}_P = (\bar{s}Rb)(\bar{\ell}\gamma_5\ell')$, and $\mathcal{O}'_{S,P}$ are obtained by exchanging $L \leftrightarrow R$. The scalar Wilson coefficients at NP scale in alignment limit are given by,

$$C_{S,P} = \frac{\rho_{sb}}{4}\left(\frac{\rho_{\ell\ell'} \pm \rho^*_{\ell'\ell}}{m_H^2} - \frac{\rho_{\ell\ell'} \mp \rho^*_{\ell'\ell}}{m_A^2}\right), \tag{20}$$

$$C'_{S,P} = \frac{\rho^*_{bs}}{4}\left(\frac{\rho_{\ell\ell'} \pm \rho^*_{\ell'\ell}}{m_H^2} + \frac{\rho_{\ell\ell'} \mp \rho^*_{\ell'\ell}}{m_A^2}\right). \tag{21}$$

Note that under $\rho_{\ell\ell'} = \rho_{\ell'\ell}$ condition, for each $C^{(\prime)}_{S,P}$ the H and A contributions are not simultaneously present.

That down-type couplings ρ_{bq}, ρ_{qb} can be finite and allowed from various flavor and collider constraints has been discussed [99] for $h \to bq$ decays in g2HDM. The most important constraints on ρ_{bq} couplings come from neutral B_q mixings, which are now induced at tree-level. Ref. [99] pointed out an effective mechanism where if one imposes the conditions $\rho_{bq}\rho_{qb} = 0$ and $m_A = m_h m_H/\sqrt{m_h^2 s_\gamma^2 + m_H^2 c_\gamma^2}$, NP effects in B_q mixing can be easily evaded. However, note that the latter condition in the alignment limit implies $m_A = m_H$, which would rule out the possibility to explain the muon $g-2$ anomaly [Eq. (17)]. Therefore, one must confront B_q mixing constraints in scenarios with $\Delta m \neq 0$.

The couplings ρ_{bq}, ρ_{qb} via tree-level H/A exchange generate the effective Hamiltonian,

$$-\mathcal{H}_{\mathrm{eff}} = C_2 O_2 + C_2' O_2' + C_4 O_4, \tag{22}$$

where the Wilson coefficients at NP scale in alignment limit are given by,

$$C_2 = \frac{\rho^{*2}_{bs}}{4}\left(\frac{1}{m_H^2} - \frac{1}{m_A^2}\right), \quad C_4 = \frac{\rho^*_{bs}\rho_{sb}}{2}\left(\frac{1}{m_H^2} + \frac{1}{m_A^2}\right), \tag{23}$$

with C_2' obtained after substituting $\rho^*_{bs} \to \rho_{sb}$ in C_2.

In Fig. 5, we show the 95% C.L. allowed region by ΔM_s measurement [Eq. (14)] for $\Delta m = 40$ GeV (blue) and 200 GeV (orange). One sees that, so long the product $\rho_{bs}\rho_{sb}$ is very small (but finite), constraints on individual couplings ρ_{bs} or ρ_{sb} can be evaded (similar results follow for ρ_{bd}, ρ_{db} from B_d mixing). Note, however, that if either ρ_{bs} or ρ_{sb} is zero, i.e. with $\rho_{bs}\rho_{sb}$ exactly zero, then the size of the other coupling is severely constrained and cannot be larger than $\mathcal{O}(10^{-3})$.

Another important probe for Case II comes from H^+-induced processes. With lepton couplings fixed by 1σ solution to muon $g-2$, ρ_{qb} and ρ_{bq} couplings contribute to leptonic decays such as $M^+ \to \ell^+\nu$ via tree-level H^+ exchange, where $M = B,\ K,\ \pi$, described by the effective Hamiltonian,

[4]In Case I, ρ_{tt} together with $\rho_{\mu\mu}$ can contribute to a_μ at two-loop, but the contribution to Δa_μ is small [29], due to constraint from $gg \to H/A \to \mu\mu$ [94,95] direct search.

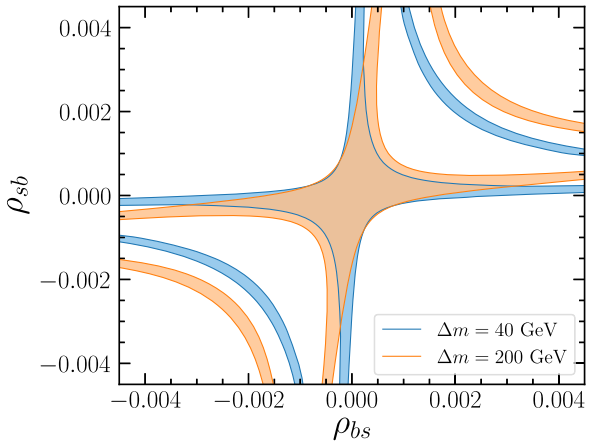

FIG. 5. Constraints from B_s mixing.

$$\mathcal{H}_{\text{eff}} = -\frac{\rho^*_{\ell'\ell}\rho^d_{kj}V_{ik}}{m^2_{H^\pm}}(\bar{u}_i R d_j)(\bar{\ell} L \nu_{\ell'}) + \text{H.c.}, \quad (24)$$

which modifies the branching ratios as follows [100],

$$\frac{\mathcal{B}(M \to \ell\bar{\nu})}{\mathcal{B}(M \to \ell\bar{\nu})_{\text{SM}}} = \sum_{\ell'}\left|\delta_{\ell\ell'} - \frac{m^2_M v^2 \rho^*_{\ell'\ell}\rho^d_{kj}V_{ik}}{2V_{u_i d_j}(m_{u_i} + m_{d_j})m_\ell m^2_{H^\pm}}\right|^2, \quad (25)$$

where m_M is the mass of meson M, and quark masses are evaluated at NP scale to account for renormalization group running. In Eq. (25), neutrino species are summed over, since neutrino flavor is not detected by experiment (the earlier work of Ref. [101] contains an error here).

Decays $B \to \mu\nu$ and $B \to \tau\nu$ provide important constraints on the coupling products $\rho_{qb}\rho_{\tau\mu}$ and $\rho_{qb}\rho_{\mu\tau}$, respectively. Adapting Eq. (25) for $B \to \mu\nu$, one notes that the SM-NP interference term (for $\ell' = \mu$) involves the coupling $\rho_{\mu\mu}$, which is strongly constrained by $\tau \to \mu\mu\mu$ [51]. Similarly, in case of $B \to \tau\nu$, the SM-interference term involves the coupling $\rho_{\tau\tau}$, which gets constrained by $\tau \to \mu\gamma$ [51]. We therefore ignore the SM-NP interference term and focus on contributions of the coupling product $\rho_{qb}\rho_{\tau\mu}$ ($\rho_{qb}\rho_{\mu\tau}$), which contribute through the incoherent term in $\mathcal{B} \to \mu\nu$ ($\mathcal{B} \to \tau\nu$).

With current values of $\mathcal{B}(B \to \mu\bar{\nu}) = (5.3 \pm 2.0 \pm 0.9) \times 10^{-7}$ [102] and $\mathcal{B}(B \to \tau\bar{\nu}) = (1.09 \pm 0.24) \times 10^{-4}$ [24], we find the ratio $R^{\mu\tau}_B = \mathcal{B}(B \to \mu\nu)/\mathcal{B}(B \to \tau\nu)$ provides a better probe compared to individual branching ratios, as it is free from parametric uncertainties such as CKM elements and decay constant. In SM, one has $R^{\mu\tau}_B(\text{SM}) \simeq 0.0045$ with negligible errors, and using measured branching ratios, we obtain $R^{\mu\tau}_B(\text{exp}) = 0.0049 \pm 0.0023$. This value for $m_{H^+} = 340$ GeV gives $|\rho_{sb}\rho_{\tau\mu}| \lesssim 6.8 \times 10^{-4}$, and $|\rho_{db}\rho_{\tau\mu}| \lesssim 1.55 \times 10^{-4}$. With $\rho_{\tau\mu} = \rho_{\mu\tau} = 0.3$ needed for 1σ solution to Δa_μ, the coupling ρ_{qb} is strongly constrained. But note that ρ_{bq} remains unconstrained by $B \to \ell\nu$. Since B_q mixing is ambivalent about which couplings, ρ_{qb} or ρ_{bq}, is large, $B \to \ell\nu$ helps remove this ambiguity. That is, the coupling ρ_{bq}, compared to ρ_{qb}, is better suited for enhancing LFV B decays.

It is worth mentioning that the ratio $R^{\mu\tau}_B$ in 2HDM Type-II (such as in minimal supersymmetric models) is lepton flavor independent and therefore remains the same as in SM. Therefore, the ratio $R^{\mu\tau}_B$ is one of the most important observables to probe genuine NP effects of g2HDM couplings [100]. We mention in passing that constraints from other decays such as $K, D \to \mu\nu$ and $\tau \to (K, \pi)\nu$ do not impose any significant bounds.

Before presenting our results, we mention few important collider probes of Scenario II. As noted in Ref. [99], if quark coupling ρ_{bs} is large then pseudoscalar A produced via strange-quark sea, i.e., $sg \to bA$, followed by $A \to bs$ is one of the best channel to search for. However, $\rho_{bs} \sim \mathcal{O}(10^{-3})$ is very small in our setup. But lepton couplings $\rho_{\tau\mu} = \rho_{\mu\tau}$ are quite large. Then exotic scalars H, A can be probed with 4-lepton final state (especially, the same-sign dimuon and same-sign ditau) via electroweak scalar pair production: $qq \to AH \to \mu^\pm\mu^\pm\tau^\mp\tau^\mp$, as pointed out in Ref. [103]. If the scalar pair is HH^+, AH^+ (or H^+H^-) then 3-lepton plus neutrino (2-lepton plus 2 neutrinos) are also channels to search for (see Ref. [103] for detail). Another potential channel could be $bs \to H, A \to \mu\tau$. Due to very small ρ_{bs} the production cross-section of H, A at LHC is expected to be small, but given that strange quark is involved, and that we also have sizable $\rho_{\tau\mu} = \rho_{\mu\tau}$, it is not clear if this constraint can be ignored. We leave a detailed analysis of collider signatures of scenario II as future work.

In Fig. 6, we present various LFV B decays as functions of $\rho_{\tau\mu}$ for a range of ρ_{bq} values, while setting $\rho_{qb} = 0$. The upper (lower) row shows results for $b \to s\tau\mu (b \to d\tau\mu)$ related decays. Note that decays $B_q \to \ell\ell'$ depend on the difference $C_i - C'_i$, $i = S, P$ scalar Wilson coefficients, while semileptonic decays $B \to (K, \pi)\ell\ell'$ depend on the sum $C_i + C'_i$ (see Appendix). But since $C_{S,P}$ vanish because $\rho_{qb} = 0$, only $C'_{S,P}$ contribute. Thus, $B_q \to \ell\ell'$ and $B \to (K, \pi)\ell\ell'$ rates are correlated, as reflected in Fig. 6, where both modes are indicated for the y axis. The dark green band in each plot corresponds to the region ruled out by current leptonic bounds. The light green region will be probed in the near future, according to Table I.[5]

We have not shown experimental sensitivity of semileptonic decays as leptonic modes appear to be the leading probe. The plots show that, for $\rho_{bq} \sim \mathcal{O}(10^{-3})$ and

[5]For $B_s \to \tau^\pm\mu^\mp$, due to lack of public results, we have conservatively assumed that future measurements can improve current limit at least by a factor of 2.

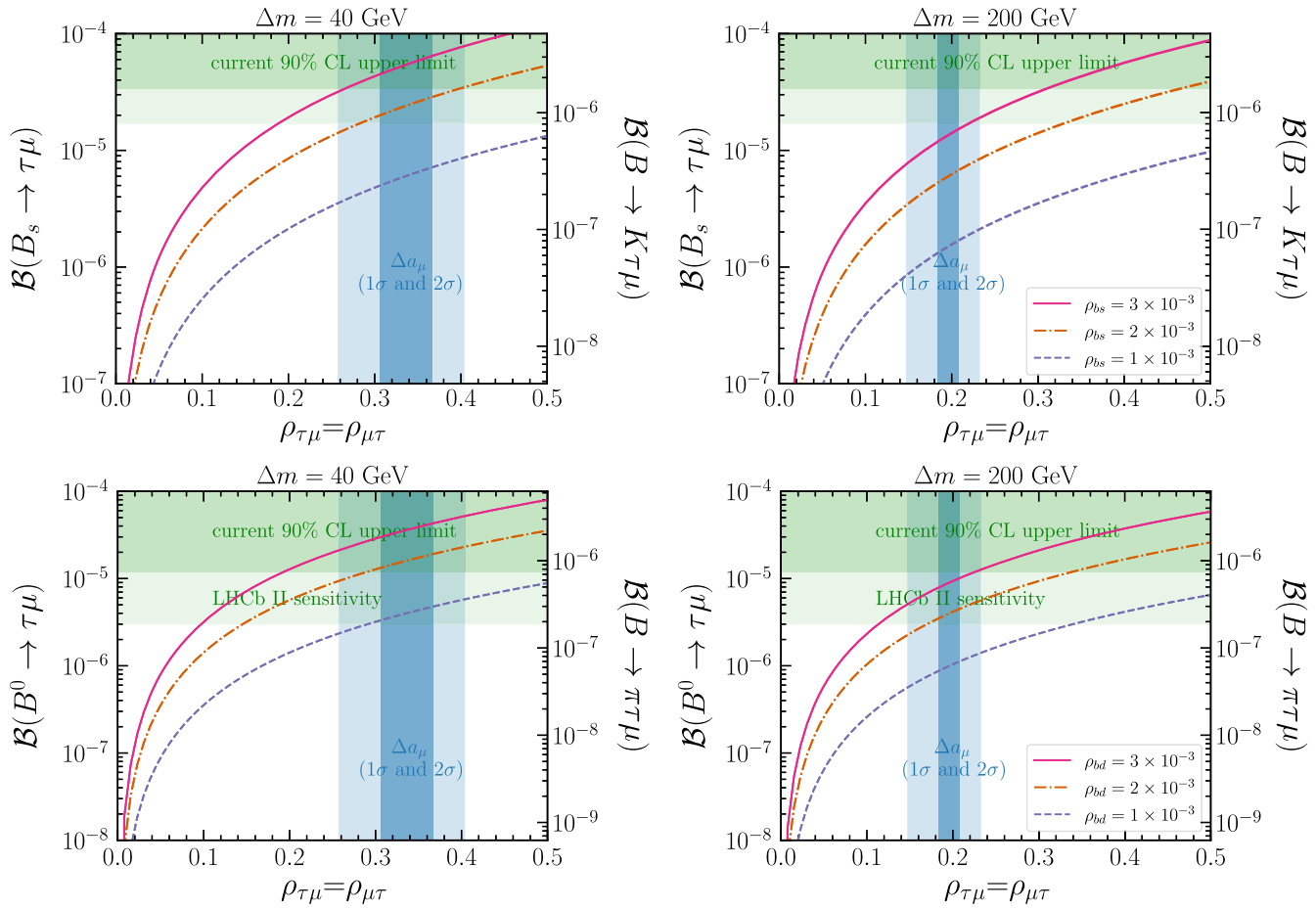

FIG. 6. Prediction for branching ratio of various LFV B decays.

$\rho_{\tau\mu} \sim \mathcal{O}(20)\lambda_\tau$ as motivated by the muon $g-2$ anomaly, large rates of LFV B decays are possible and within reach of future searches. One also notes from Fig. 6 that scenarios with smaller mass splitting $\Delta m < 200$ GeV have better prospects for discovery, although the needed $\rho_{\tau\mu}$ value is larger, hence somewhat less attractive.

Let us now briefly comment on τ–e and μ–e sectors. The B decays with $\tau - e$ flavor violation involve $\rho_{\tau e}$ and $\rho_{e\tau}$ couplings, but $\mu \to e\gamma$ puts a strong bound on them. The corresponding contribution to $\mu \to e\gamma$ is generated by a diagram similar to Fig. 4, but with outgoing fermion replaced by electron. For values of $\rho_{\tau\mu}, \rho_{\mu\tau}$ that explain

TABLE I. Summary of current experimental data on LFV B decays considered in our analysis.

Decay mode	90% C.L. Upper Limit	Future sensitivity
$B_s \to \tau^\pm\mu^\mp$	3.4×10^{-5} (LHCb [13])	⋯
$B_d \to \tau^\pm\mu^\mp$	1.2×10^{-5} (LHCb [13])	3×10^{-6} (LHCb II [14])
$B^+ \to K^+\tau^+\mu^-$	2.8×10^{-5} (*BABAR* [15])	$\sim 3 \times 10^{-6}$ (Belle II [16])
$B^+ \to \pi^+\tau^+\mu^-$	4.5×10^{-5} (*BABAR* [15])	⋯
$B_d \to \tau^\pm e^\mp$	1.6×10^{-5} (Belle [17])	⋯
$B^+ \to K^+\tau^+e^-$	1.5×10^{-5} (*BABAR* [15])	$\sim 2 \times 10^{-6}$ (Belle II [16])
$B^+ \to \pi^+\tau^+e^-$	2.0×10^{-5} (*BABAR* [15])	⋯
$B_s \to \mu^\pm e^\mp$	5.4×10^{-9} (LHCb [18])	3×10^{-10} (LHCb II [14])
$B_d \to \mu^\pm e^\mp$	1.0×10^{-9} (LHCb [18])	9×10^{-11} (LHCb II [14])
$B^+ \to K^+\mu^+e^-$	6.4×10^{-9} (LHCb [19])	⋯
$B^+ \to \pi^+e^\pm\mu^\mp$	1.7×10^{-7} (*BABAR* [20])	⋯

the $(g-2)_\mu$ anomaly, the MEG bound of $\mu \to e\gamma < 4.2 \times 10^{-13}$ [50] would imply $\rho_{\tau e} = \rho_{e\tau} \lesssim \mathcal{O}(\lambda_e)$ [51], which is quite severe. Therefore, to avoid the charged LFV constraint, we take $\rho_{\tau e} = \rho_{e\tau} \sim \lambda_e$. Then predictions with $\rho_{bq} = 10^{-3}$, $m_H = 300\,\text{GeV}$, $m_A = 340$ GeV are $\mathcal{B}(B_s \to \tau e) \sim 5 \times 10^{-16}$, $\mathcal{B}(B \to K\tau e) \sim 10^{-17}$ and $\mathcal{B}(B_d \to \tau e) \sim 3 \times 10^{-16}$, $\mathcal{B}(B \to \pi\tau e) \sim 10^{-17}$, which are far below future sensitivities.

We find the coupling of the $\mu - e$ sector only weakly constrained in Case II by charged LFV processes. The couplings $\rho_{\mu\tau}$, $\rho_{\tau\mu}$ together with $\rho_{\mu e}$, $\rho_{e\mu}$ contribute to $\tau \to e\gamma$ via diagrams similar to Fig. 4, after replacing initial and final fermions by τ and e and internal fermion by μ. But the diagram is chirally suppressed by small m_μ. Taking same mass as before and $\rho_{e\mu} = \rho_{\mu e}$, the current measurement of $\mathcal{B}(\tau \to e\gamma) = 3.3 \times 10^{-8}$ [49] sets the bound $\rho_{\tau\mu}\rho_{\mu e} \lesssim (5 \times 10^5)\lambda_\tau\lambda_e$, which is quite poor. Note that $\tau^- \to \mu^- e^+ \mu^-$ gives better constraint, as this decay is mediated by tree-level H, A exchange hence does not suffer chiral suppression. Adapting the formula of $\tau^- \to \mu^-\mu^+\mu^-$ given in Ref. [101] to $\tau^- \to \mu^- e^+ \mu^-$, we find an order of magnitude improvement in constraint on $\rho_{\tau\mu}\rho_{\mu e}$ compared to $\tau \to e\gamma$. Then taking $\rho_{e\mu} = \rho_{\mu e} \sim 10^3\lambda_e (\simeq 0.003)$ and $\rho_{bq} = 10^{-3}$ with $m_H = 300$ GeV and $m_A = 340$ GeV, we find $\mathcal{B}(B_s \to \mu e) \sim 6 \times 10^{-10}$, $\mathcal{B}(B \to K\mu e) \sim 3 \times 10^{-11}$ and $\mathcal{B}(B_d \to \mu e) \sim 4 \times 10^{-10}$, $\mathcal{B}(B \to \pi\mu e) \sim 3 \times 10^{-11}$. These values can be probed in the near future.

V. SUMMARY

We have explored prospects of enhanced lepton flavor violation in B decays in g2HDM with sub-TeV exotic scalars. We focus on two different cases of parameter space. For Case I, we assume the top Yukawa coupling ρ_{tt} is the dominant quark coupling and take $c_\gamma \sim 0.1$. Then charged LFV processes $\tau \to \mu\gamma$ and $\mu \to e\gamma$ constrain $\rho_{\ell\ell'}$ to Eq. (5). Even with $\mathcal{O}(1)$ strength of ρ_{tt}, LFV B decay rates are highly suppressed by small $\rho_{\ell\ell'}$, and are far from the sensitivities of upcoming LHCb Upgrade II and Belle II. For Case II where μ–τ flavor violating lepton couplings are motivated to be about 20-30 times larger than SM Yukawa $\lambda_\tau \simeq 0.01$. Contrary to Case I, one finds that ρ_{tt} has to be small due to bounds from $\tau \to \mu\gamma$ and $gg \to H, A \to \tau\mu$ direct search at LHC. However, together with ρ_{bs}, ρ_{bd} as small as $\mathcal{O}(10^{-3})$, we find that Case II allows substantial rates of μ–τ flavor violation in B decays, with B mixing and $B \to \mu\nu$ being the leading, but forgiving, flavor constraints.

Concerning τ–e flavor violation in B decays, we find that $\mu \to e\gamma$ would make it difficult to have simultaneously large $\rho_{\tau e}$, making $B_q \to \tau e$ and $B \to (K, \pi)\tau e$ rates too small to be probed at upcoming experiments. Furthermore, we find that current constraints on μ–e flavor violating coupling are not that severe. The future measurements of LFV B decays related to $b \to q\mu e$ will provide crucial constraint on g2HDM.

ACKNOWLEDGMENTS

This work is supported by NSTC Grant No. 111-2639-M-002-002-ASP of Taiwan, and NTU Grants No. 111L104019 and No. 111L894801.

APPENDIX: USEFUL FORMULAS

1. The T-parameter

The parameter in g2HDM is defined as [42,43]

$$\begin{aligned} T = \frac{1}{16\pi s_W^2 m_W^2}\{ & F(m_A^2, m_{H^+}^2) + c_\gamma^2[F(m_{H^+}^2, m_h^2 - F(m_A^2, m_h^2)] \\ & + s_\gamma^2[F(m_{H^+}^2, m_H^2) - F(m_A^2, m_H^2)] \\ & - 3c_\gamma^2[F(m_Z^2, m_h^2) - F(m_W^2, m_h^2) \\ & + F(m_W^2, m_H^2) - F(m_Z^2, m_H^2)]\}, \end{aligned} \tag{A1}$$

where function $F(a, b)$ is given by

$$F(a, b) = \frac{a+b}{2} - \frac{ab}{a-b}\log\frac{1}{b}, \tag{A2}$$

which vanishes in the limit $a \to b$.

2. $h \to \ell\ell^{(\prime)}$

The tree-level decay rate for $h \to \ell\ell'$ $(\ell \neq \ell')$ is,

$$\begin{aligned} \Gamma(h \to \ell\ell') &= \Gamma(h \to \ell^+\ell'^-) + \Gamma(h \to \ell^-\ell'^+) \\ &\approx \frac{c_\gamma^2 m_h}{16\pi}(|\rho_{\ell\ell'}|^2 + |\rho_{\ell'\ell}|^2), \end{aligned} \tag{A3}$$

and for flavor conserving case,

$$\frac{\Gamma(h \to \ell\ell)}{\Gamma(h \to \ell\ell)_{\text{SM}}} \approx \left| s_\gamma + c_\gamma \text{Re}\frac{\rho_{\ell\ell}}{\lambda_\ell} \right|^2 + \left| c_\gamma \text{Im}\frac{\rho_{\ell\ell}}{\lambda_\ell} \right|^2. \tag{A4}$$

3. $B \to \ell\ell^{(\prime)}$, $B \to M\ell\ell^{(\prime)}$ $(M = K, \pi)$

The effective Hamiltonian for $b \to q\ell\ell^{(\prime)}$ is,

$$\mathcal{H}_{\text{eff}} = -\frac{4G_F}{\sqrt{2}} V_{tq}^* V_{tb} \frac{e^2}{16\pi^2} \sum (C_i O_i + C_i' O_i'), \tag{A5}$$

with relevant operators,

$$O_7 = \frac{m_b}{e}(\bar{s}\sigma^{\mu\nu}Rb)F_{\mu\nu}, \qquad O_8 = \frac{g_s^2}{e^2}m_b(\bar{s}\sigma^{\mu\nu}T^aRb)G^a_{\mu\nu},$$
$$O_9 = (\bar{s}\gamma_\mu Lb)(\bar{\ell}\gamma^\mu\ell), \qquad O_{10} = (\bar{s}\gamma_\mu Lb)(\bar{\ell}\gamma^\mu\gamma_5\ell),$$
$$O_S = (\bar{s}Rb)(\bar{\ell}\ell), \qquad O_P = (\bar{s}Rb)(\bar{\ell}\gamma_5\ell), \tag{A6}$$

where primed counterparts are obtained by $L \to R$ exchange. The full $b \to q\ell\ell$ operator basis can be found, e.g., in Refs. [104–106]. One should take note of the normalization used in $\mathcal{H}_{\rm eff}$ in Eq. (A5) when comparing with $\mathcal{H}_{\rm eff}$ defined in Eqs. (6) and (19) in the main text.

With NP operators of Eq. (A6), $\mathcal{B}(B_s \to \ell\ell')$ with respect to SM is given by [107]

$$\mathcal{B}(B_q \to \ell\ell^{(\prime)}) = \frac{G_F^2\alpha^2|V_{tq}^*V_{tb}|^2 f_{B_q}^2\tau_{B_q}}{64\pi^3 m_{B_q}^3}\lambda^{\frac{1}{2}}(m_{B_q}, m_\ell, m_{\ell'}) \times \left\{(m_{B_q}^2 - m_+^2)|\Delta C_9 m_- + \Delta C_S\frac{m_{B_q}^2}{m_b+m_q}|^2 + (m_{B_q}^2 - m_-^2)|\Delta C_{10}m_+ + \Delta C_P\frac{m_{B_q}^2}{m_b+m_q}|^2\right\}, \tag{A7}$$

where $\lambda(a,b,c) = [a^2-(b-c)^2][a^2-(b+c)^2]$, and $m_\pm = m_\ell \pm m_{\ell'}$, $\Delta C_i = C_i - C_i'$. For $\ell = \ell'$, C_9 vanishes due to Ward identity for on-shell leptons.

The differential branching ratio of $B \to (K,\pi)\ell\ell^{(\prime)}$ is

$$d\mathcal{B}(B \to M\ell\ell^{(\prime)})/dq^2 = |\mathcal{N}_M(q^2)|^2\left\{\sum_i \varphi_i(q^2)|C_i + C_i'|^2 + \sum_{(i,j)}\varphi_{ij}(q^2)\mathrm{Re}[(C_i+C_i')(C_j+C_j')^*]\right\}, \tag{A8}$$

where q is the B to M momentum transfer, and i and (i,j) run over $\{7,9,10,S,P\}$ and $\{(7,9),(9,S),(10,P)\}$, respectively. The functions $\mathcal{N}_M(q^2)$ and $\varphi_{i(j)}(q^2)$ are given in Ref. [107] (also see Ref. [108] for a general formalism of semileptonic B decays).

4. $b \to s\gamma$

The H^+ induced dipole coefficients C_7 and C_8 mediating $b \to s\gamma$ and $b \to sg$ in g2HDM are given by,

$$\delta C_{7(8)}(x_t) = \frac{|\rho_{tt}|^2}{3|\lambda_t|^2}F_{7(8)}^{(1)}(x_t), \tag{A9}$$

where the loop functions $F_{7(8)}^{(1)}(x)$ are in the notation of Ref. [109] (originally calculated in Ref. [110]) and provided in the next appendix.

5. Loop functions

Loop functions related to $\Delta B = 1$ decays [111] and $|\Delta B| = 2$ processes are [25,58] are listed below.

$$G_Z(a) = \frac{a(1-a+\log a)}{2(1-a)^2},$$
$$G_\gamma(a) = -\frac{2(16-45a+36a^2-7a^3+6(2-3a)\log a)}{108(1-a)^4} - \frac{2-9a+18a^2-11a^3+6a^3\log a}{36(1-a)^4}, \tag{A10}$$
$$F_7^{(1)}(a) = \frac{a(7-5a-8a^2)}{24(a-1)^3} + \frac{a^2(3a-2)}{4(a-1)^4}\log a, \tag{A11}$$
$$F_8^{(1)}(a) = \frac{a(2+5a-a^2)}{8(a-1)^3} - \frac{3a^2}{4(a-1)^4}\log a, \tag{A12}$$
$$f(a) = -\frac{1+a}{(a-1)^2} + \frac{2a\log a}{(a-1)^3}, \tag{A13}$$
$$g(a,b) = \frac{1}{(a-b)^2}\left[-\frac{3a^2\log a}{a-1} + \frac{(b-4a)(b-a)}{b-1} + \frac{(-4a^2+3ab^2+2ab-b^2)\log b}{(b-1)^2}\right]. \tag{A14}$$

[1] S. L. Glashow, J. Iliopoulos, and L. Maiani, Phys. Rev. D **2**, 1285 (1970).
[2] Y. Aoki, T. Blum, G. Colangelo, S. Collins, M. Della Morte, P. Dimopoulos, S. Dürr, X. Feng, H. Fukaya, M. Golterman *et al.*, Eur. Phys. J. C **82**, 869 (2022).
[3] R. Aaij *et al.* (LHCb Collaboration), Phys. Rev. Lett. **128**, 041801 (2022).
[4] R. Aaij *et al.* (LHCb Collaboration), Phys. Rev. D **105**, 012010 (2022).
[5] CMS Collaboration, arXiv:2212.10311.
[6] C. Bobeth, M. Gorbahn, T. Hermann, M. Misiak, E. Stamou, and M. Steinhauser, Phys. Rev. Lett. **112**, 101801 (2014).
[7] M. Beneke, C. Bobeth, and R. Szafron, J. High Energy Phys. 10 (2019) 232.
[8] S. L. Glashow, D. Guadagnoli, and K. Lane, Phys. Rev. Lett. **114**, 091801 (2015).
[9] L. Calibbi, A. Crivellin, and T. Ota, Phys. Rev. Lett. **115**, 181801 (2015).
[10] F. Feruglio, P. Paradisi, and A. Pattori, Phys. Rev. Lett. **118**, 011801 (2017).
[11] LHCb Collaboration, arXiv:2212.09152.
[12] LHCb Collaboration, arXiv:2212.09153.
[13] R. Aaij *et al.* (LHCb Collaboration), Phys. Rev. Lett. **123**, 211801 (2019).
[14] R. Aaij *et al.* (LHCb Collaboration), arXiv:1808.08865.
[15] J. P. Lees *et al.* (*BABAR* Collaboration), Phys. Rev. D **86**, 012004 (2012).
[16] E. Kou *et al.* (Belle-II Collaboration), Prog. Theor. Exp. Phys. **2019**, 123C01 (2019); **2020**, 029201(E) (2020).
[17] H. Atmacan *et al.* (Belle Collaboration), Phys. Rev. D **104**, L091105 (2021).
[18] R. Aaij *et al.* (LHCb Collaboration), J. High Energy Phys. 03 (2018) 078.
[19] R. Aaij *et al.* (LHCb Collaboration), Phys. Rev. Lett. **123**, 241802 (2019).
[20] B. Aubert *et al.* (*BABAR* Collaboration), Phys. Rev. Lett. **99**, 051801 (2007).
[21] T. D. Lee, Phys. Rev. D **8**, 1226 (1973).
[22] G. C. Branco, P. M. Ferreira, L. Lavoura, M. N. Rebelo, M. Sher, and J. P. Silva, Phys. Rep. **516**, 1 (2012).
[23] W.-S. Hou, Phys. Lett. B **296**, 179 (1992).
[24] P. A. Zyla *et al.* (Particle Data Group), Prog. Theor. Exp. Phys. **2020**, 083C01 (2020).
[25] W.-S. Hou and G. Kumar, Phys. Rev. D **102**, 115017 (2020).
[26] K. Fuyuto, W.-S. Hou, and E. Senaha, Phys. Lett. B **776**, 402 (2018).
[27] K. Fuyuto, W.-S. Hou, and E. Senaha, Phys. Rev. D **101**, 011901 (2020).
[28] B. Abi *et al.* (Muon g-2 Collaboration), Phys. Rev. Lett. **126**, 141801 (2021).
[29] W.-S. Hou, R. Jain, C. Kao, G. Kumar, and T. Modak, Phys. Rev. D **104**, 075036 (2021).
[30] H. Georgi and D. V. Nanopoulos, Phys. Lett. **82B**, 95 (1979).
[31] L. Lavoura and J. P. Silva, Phys. Rev. D **50**, 4619 (1994).
[32] F. J. Botella and J. P. Silva, Phys. Rev. D **51**, 3870 (1995).
[33] S. Davidson and H. E. Haber, Phys. Rev. D **72**, 035004 (2005); **72**, 099902(E) (2005).
[34] F. Mahmoudi and O. Stal, Phys. Rev. D **81**, 035016 (2010).
[35] S. L. Glashow and S. Weinberg, Phys. Rev. D **15**, 1958 (1977).
[36] W.-S. Hou and M. Kikuchi, Europhys. Lett. **123**, 11001 (2018).
[37] T. Aaltonen *et al.* (CDF Collaboration), Science **376**, 170 (2022).
[38] H. Bahl, J. Braathen, and G. Weiglein, Phys. Lett. B **833**, 137295 (2022).
[39] H. Song, W. Su, and M. Zhang, J. High Energy Phys. 10 (2022) 048.
[40] K. S. Babu, S. Jana, and V. P. K., Phys. Rev. Lett. **129**, 121803 (2022).
[41] F. Arco, S. Heinemeyer, and M. J. Herrero, Phys. Lett. B **835**, 137548 (2022).
[42] D. O'Neil, arXiv:0908.1363.
[43] S. Davidson and G. J. Grenier, Phys. Rev. D **81**, 095016 (2010).
[44] D. K. Ghosh, W.-S. Hou, and T. Modak, Phys. Rev. Lett. **125**, 221801 (2020).
[45] T.-P. Cheng and M. Sher, Phys. Rev. D **35**, 3484 (1987).
[46] A. M. Sirunyan *et al.* (CMS Collaboration), Phys. Rev. D **104**, 032013 (2021).
[47] S. M. Barr and A. Zee, Phys. Rev. Lett. **65**, 21 (1990); **65**, 2920(E) (1990).
[48] A. Abdesselam *et al.* (Belle Collaboration), J. High Energy Phys. 10 (2021) 019.
[49] B. Aubert *et al.* (*BABAR* Collaboration), Phys. Rev. Lett. **104**, 021802 (2010).
[50] A. M. Baldini *et al.* (MEG Collaboration), Eur. Phys. J. C **76**, 434 (2016).
[51] W.-S. Hou and G. Kumar, Eur. Phys. J. C **81**, 1132 (2021).
[52] G. Aad *et al.* (ATLAS Collaboration), Phys. Lett. B **812**, 135980 (2021).
[53] A. M. Sirunyan *et al.* (CMS Collaboration), J. High Energy Phys. 01 (2021) 148.
[54] A. Tumasyan *et al.* (CMS Collaboration), J. High Energy Phys. 06 (2022) 012.
[55] W.-S. Hou, G. Kumar, and S. Teunissen, J. High Energy Phys. 01 (2022) 092.
[56] J. Baron *et al.* (ACME Collaboration), Science **343**, 269 (2014).
[57] V. Andreev *et al.* (ACME Collaboration), Nature (London) **562**, 355 (2018).
[58] A. Crivellin, D. Müller, and C. Wiegand, J. High Energy Phys. 06 (2019) 119.
[59] D. M. Straub, arXiv:1810.08132.
[60] J. Aebischer, J. Kumar, and D. M. Straub, Eur. Phys. J. C **78**, 1026 (2018).
[61] L. Di Luzio, M. Kirk, A. Lenz, and T. Rauh, J. High Energy Phys. 12 (2019) 009.
[62] W.-S. Hou and G. Kumar, J. High Energy Phys. 10 (2022) 129.
[63] G. W. Bennett *et al.* (Muon g-2 Collaboration), Phys. Rev. D **73**, 072003 (2006).
[64] T. Aoyama *et al.*, Phys. Rep. **887**, 1 (2020).
[65] T. Aoyama, M. Hayakawa, T. Kinoshita, and M. Nio, Phys. Rev. Lett. **109**, 111808 (2012).
[66] T. Aoyama, T. Kinoshita, and M. Nio, Atoms **7**, 28 (2019).

[67] A. Czarnecki, W. J. Marciano, and A. Vainshtein, Phys. Rev. D **67**, 073006 (2003); **73**, 119901(E) (2006).
[68] C. Gnendiger, D. Stöckinger, and H. Stöckinger-Kim, Phys. Rev. D **88**, 053005 (2013).
[69] M. Davier, A. Hoecker, B. Malaescu, and Z. Zhang, Eur. Phys. J. C **77**, 827 (2017).
[70] M. Davier, A. Hoecker, B. Malaescu, and Z. Zhang, Eur. Phys. J. C **71**, 1515 (2011); **72**, 1874(E) (2012).
[71] A. Keshavarzi, D. Nomura, and T. Teubner, Phys. Rev. D **97**, 114025 (2018).
[72] G. Colangelo, M. Hoferichter, and P. Stoffer, J. High Energy Phys. 02 (2019) 006.
[73] M. Hoferichter, B. L. Hoid, and B. Kubis, J. High Energy Phys. 08 (2019) 137.
[74] M. Davier, A. Hoecker, B. Malaescu, and Z. Zhang, Eur. Phys. J. C **80**, 241 (2020); **80**, 410(E) (2020).
[75] A. Keshavarzi, D. Nomura, and T. Teubner, Phys. Rev. D **101**, 014029 (2020).
[76] A. Kurz, T. Liu, P. Marquard, and M. Steinhauser, Phys. Lett. B **734**, 144 (2014).
[77] K. Melnikov and A. Vainshtein, Phys. Rev. D **70**, 113006 (2004).
[78] P. Masjuan and P. Sanchez-Puertas, Phys. Rev. D **95**, 054026 (2017).
[79] G. Colangelo, M. Hoferichter, M. Procura, and P. Stoffer, J. High Energy Phys. 04 (2017) 161.
[80] M. Hoferichter, B. L. Hoid, B. Kubis, S. Leupold, and S. P. Schneider, J. High Energy Phys. 10 (2018) 141.
[81] A. Gérardin, H. B. Meyer, and A. Nyffeler, Phys. Rev. D **100**, 034520 (2019).
[82] J. Bijnens, N. Hermansson-Truedsson, and A. Rodríguez-Sánchez, Phys. Lett. B **798**, 134994 (2019).
[83] G. Colangelo, F. Hagelstein, M. Hoferichter, L. Laub, and P. Stoffer, J. High Energy Phys. 03 (2020) 101.
[84] T. Blum, N. Christ, M. Hayakawa, T. Izubuchi, L. Jin, C. Jung, and C. Lehner, Phys. Rev. Lett. **124**, 132002 (2020).
[85] G. Colangelo, M. Hoferichter, A. Nyffeler, M. Passera, and P. Stoffer, Phys. Lett. B **735**, 90 (2014).
[86] S. Borsanyi *et al.*, Nature (London) **593**, 51 (2021).
[87] M. Cè *et al.*, Phys. Rev. D **106**, 114502 (2022).
[88] C. Alexandrou *et al.*, Phys. Rev. D **107**, 074506 (2023).
[89] T. Blum *et al.*, arXiv:2301.08696.
[90] A. Bazavov *et al.*, arXiv:2301.08274.
[91] A. Crivellin, M. Hoferichter, C. A. Manzari, and M. Montull, Phys. Rev. Lett. **125**, 091801 (2020).
[92] A. Keshavarzi, W. J. Marciano, M. Passera, and A. Sirlin, Phys. Rev. D **102**, 033002 (2020).
[93] G. Colangelo, M. Hoferichter, and P. Stoffer, Phys. Lett. B **814**, 136073 (2021).
[94] A. M. Sirunyan *et al.* (CMS Collaboration), Phys. Lett. B **798**, 134992 (2019).
[95] M. Aaboud *et al.* (ATLAS Collaboration), J. High Energy Phys. 07 (2019) 117.
[96] K. A. Assamagan, A. Deandrea, and P. A. Delsart, Phys. Rev. D **67**, 035001 (2003).
[97] Y. Omura, E. Senaha, and K. Tobe, Phys. Rev. D **94**, 055019 (2016).
[98] A. M. Sirunyan *et al.* (CMS Collaboration), J. High Energy Phys. 03 (2020) 103.
[99] A. Crivellin, J. Heeck, and D. Müller, Phys. Rev. D **97**, 035008 (2018).
[100] W.-S. Hou, M. Kohda, T. Modak, and G.-G. Wong, Phys. Lett. B **800**, 135105 (2020).
[101] A. Crivellin, A. Kokulu, and C. Greub, Phys. Rev. D **87**, 094031 (2013).
[102] M. T. Prim *et al.* (Belle Collaboration), Phys. Rev. D **101**, 032007 (2020).
[103] S. Iguro, Y. Omura, and M. Takeuchi, J. High Energy Phys. 11 (2019) 130.
[104] B. Grinstein, M. J. Savage, and M. B. Wise, Nucl. Phys. **B319**, 271 (1989).
[105] G. Buchalla, A. J. Buras, and M. E. Lautenbacher, Rev. Mod. Phys. **68**, 1125 (1996).
[106] K. G. Chetyrkin, M. Misiak, and M. Munz, Phys. Lett. B **400**, 206 (1997); **425**, 414(E) (1998).
[107] D. Bečirević, O. Sumensari, and R. Zukanovich Funchal, Eur. Phys. J. C **76**, 134 (2016).
[108] J. Gratrex, M. Hopfer, and R. Zwicky, Phys. Rev. D **93**, 054008 (2016).
[109] M. Ciuchini, G. Degrassi, P. Gambino, and G. F. Giudice, Nucl. Phys. **B527**, 21 (1998).
[110] W.-S. Hou and R. S. Willey, Phys. Lett. B **202**, 591 (1988).
[111] S. Iguro and K. Tobe, Nucl. Phys. **B925**, 560 (2017).